TAPROBANICA, ISSN 1800–427X. November, 2023. Vol. 12, No. 02: pp. 48–58, pl. 22–24.

http://www.taprobanica.org
https://doi.org/10.47605/tapro.v12i2.307

urn:lsid:zoobank.org:pub:688A1A2E-D972-45D6-B5F7-9AE851FA03D9

A NEW DWARF GECKO SPECIES (SQUAMATA: GEKKONIDAE: *Cnemaspis*) FROM THE NORTHERN WESTERN GHATS OF INDIA

Section Editor: Thasun Amarasinghe *Submitted*: 8 August 2023, *Accepted*: 28 October 2023

Amit Sayyed*

* *Wildlife Protection and Research Society (WLPRS), Satara, Maharashtra, India*
E-mail: amitsayyedsatara@gmail.com

Abstract
Based on molecular and morphological data, I describe a new species of the polyphyletic gekkonid genus *Cnemaspis* Strauch, 1887 from the northern Western Ghats in India. The new species is the second smallest known Indian dwarf gekkonid and belongs to the clade of *C. girii* sensu Pal *et al*. (2021). It is genetically distinct from all congeners of the *C. girii* clade by *p*-distance ranging from 3.8 to 8.4 % on the 16S rRNA gene. Morphologically, the new species can be distinguished from all congeners by having the following combination of characters: A small species with adult males reaching a maximum SVL 27.0 mm; heterogeneous dorsal pholidosis with 11–12 longitudinal rows of enlarged tubercles; males with 3–4 femoral pores on each thigh, separated medially by 19–24 poreless scales; 63–65 middorsal scales; 136–150 ventral scales; 33–35 midbody scales; 12–14 subdigital lamellae under fourth digit of pes; feebly carinate scales on the neck and chest; and absence of conical or spine-like tubercles on flank.

Keywords: dwarf geckos, *girii* clade, Maharashtra, molecular phylogeny, 16S, systematics, taxonomy

Introduction

The Northern Western Ghats (NWG), stretching across the states of Gujarat, Maharashtra, Goa and Karnataka constitute one of the most ecologically sensitive regions in India (Rodgers *et al*. 2000). Its complex topography, coupled with varying climatic conditions, has led to the creation of a mosaic of habitats that have fostered the evolution of numerous endemic species (Myers *et al*. 2000). One of the fascinating groups of geckos found in NWG belongs to the genus *Cnemaspis* Strauch, 1887, which are small sized and diurnal geckos known for their intricate patterns, remarkable adaptations, and endemism (Grismer *et al*. 2014, Khandekar *et al*. 2021a, Sayyed *et al*. 2018, 2021). Several new species in this group from NWG have been discovered in recent years (e.g., Giri *et al*. 2009, Mirza *et al*. 2014, Sayyed *et al*. 2016, 2018, 2021, Sayyed & Sulakhe 2020, Khandekar *et al*. 2019, 2021a,b).

There are 13 species of *Cnemaspis* distributed in the NWG region that are nested within three different clades, *C. goaensis* Sharma 1976, *C. wayanadensis* Beddome 1870, and *C. girii* Mirza *et al*. 2014 (Mirza *et al*. 2014, Sayyed

et al. 2016, 2018, 2021, Sayyed & Sulakhe 2020, Pal *et al*. 2021, Khandekar *et al*. 2019, 2021a, b). In this communication, I describe a new species of *Cnemaspis* from the *C. girii* clade from Gandharpale Caves in Mahad, Maharashtra, India, based on morphological and molecular data.

Material and methods

***Sampling*.** Type specimens were collected during the evening hours from Mahad, Maharashtra, India. They were collected by hand from the rock wall, photographed in life, and then euthanized using halothane following the guidelines by Leary *et al*. (2013). Thigh tissue was used for further molecular work. The specimens were subsequently fixed in 4% formaldehyde for ~24 hours, washed in water and later transferred to 70% ethanol for long term preservation. Scalation and other morphological characters were recorded using a Lensel stereo microscope. The material referred to in this study is deposited in the collection of the Bombay Natural History Society (BNHS), Mumbai, Maharashtra, India.

***Morphological data*.** Morphometric data are given as % of SVL. Morphological data were taken using a Mitutoyo 500, (to the nearest 0.1 mm). For the geographical coordinates and altitude readings, I used a Kestrel 4500 receiver. Morphological data was recorded as snout–vent length (SVL), from tip of snout to anterior margin of vent; axilla–groin length (AG), from axilla to groin; trunk width (TW), maximum width of the body; eye diameter (ED), horizontal diameter of the orbit; eye–nares distance (EN), distance between anterior point of the orbit to the posterior part of the nostril; snout length (ES), from anterior margin of the orbit to the tip of the snout; eye–ear distance (ET), from posterior margin of the orbit to the anterior margin of the ear opening; internarial distance (IN), least distance between the inner margins of the nostrils; ear opening diameter (EOD), horizontal distance from the anterior to posterior margin of the ear opening; head length (HL), from tip of snout to posterior edge of mandible; head width (HW), maximum width of the head; head depth (HD), maximum depth of the head; interorbital distance (IO), shortest distance between the superciliary scale rows; upper arm length (UAL), from axilla to elbow, lower arm length (LAL), from elbow to wrist; Finger length (FL), from the tip of the finger to the nearest fork; femur length (FEL), from groin to the knee; tibia length (TBL), from knee to heel; toe length (TOL), from tip of 1st toe to the nearest fork; tail length (TL), distance between posterior margin of vent to the tip of the tail.

Meristic data recorded for all specimens included number of supralabials and infralabials on left and right sides; number of supraciliaries; number of interorbital scales; number of scales between eye to tympanum, from posterior-most point of the orbit to anterior-most point of the tympanum; number of the postnasal, all scales posterior to the naris; number of postmentals; number of posterior postmentals, scales that are surrounded by the posterior-postmentals and between infralabials; number of supranasal, excluding the smaller scales between the larger supranasals; number of canthal scales, number of scales from posterior-most point of naris to anterior most point of the orbit; number of midbody dorsal scale rows, from the centre of middorsal row diagonally towards the ventral scales; dorsal tubercle rows, longitudinal rows of enlarged tubercles; number of midventral scales, from the first scale posterior to the mental to last scale anterior to the vent; number of scale rows across the belly, across the ventral between the lowest rows of dorsal scales; femoral pores, the number of femoral pores; poreless scales, poreless scales between right and left femur; lamellae under digits of manus and pes on right side, counted from first proximal enlarged scansor greater than twice width of the largest palm scale, to distalmost lamella at tip of digits; lamellae under fourth digit of manus.

***Molecular data*.** DNA extraction, amplification, and sequencing: DNA extraction, amplification and sequencing protocols for the 16S gene as per Sayyed *et al*. (2021) were followed. The genomic DNA of *Cnemaspis* specimens (BNHS 2927 and BNHS 2928) was extracted from muscle tissue (thigh tissue) samples that were preserved in 100% ethanol. The DNA extraction was carried out using a DNeasy (QiagenTM) blood and tissue kit following the manufacturer's instructions. Partial sequences of the mitochondrial 16S rRNA gene of the new species were amplified. The amplification of 16S was carried out in three steps using primers 16Sar and 16sbr (Simon *et al*. 1991). The fragments were amplified with the following conditions: 95°C – 3 min, 1 cycle, 95°C – 30 sec, 50°C – 30 sec, 72°C – 1 min, 35 Cycles, 72°C – 7 min. I then sequenced the forward and reverse DNA strands using a BDT v3.1 Cycle sequencing kit on ABI 3730xl Genetic Analyzer.

Sequence alignments: The 16S rRNA sequences were cleaned manually with MEGA v.7 (Kumar *et al*. 2016) using chromatograms visualised in Chromas v.2.6.5 (Technelysium Pty. Ltd.). Comparative ND2 and 16S sequences comprising members of the *Cnemaspis* genus were downloaded from GenBank following Pal *et al*. (2021), Agarwal *et al*. (2022), Narayanan & Aravind (2022), Narayanan *et al*. (2023), and Sayyed *et al*. (2023) and newly generated sequences were deposited in the GenBank® (Benson *et al*. 2017) under accession numbers as per Appendix 1. The sequences were aligned using MUSCLE (Edgar 2004) in MEGA v.7 (Tamura & Nei 1993, Kumar *et al*. 2016) with default parameter settings. The final ND2 alignment contained 112 sequences (110 ingroups and 2 outgroups) with 1039 base pair lengths whereas the 16S alignment contained 52 sequences with 588 base pair lengths. Later the ND2 and 16S datasets were concatenated and used for phylogenetic analyses due to unavailability of 16S sequence for *C. girii*. *Phelsuma ornata* Gray 1825 (EU423282) and *Phelsuma lineata* Gray 1842 (EU423283) were used as outgroups to root the phylogenetic analyses.

Molecular phylogenetics analysis: The Maximum Likelihood (ML) method of phylogenetic analyses was implemented. The ND2 region was partitioned per codon position, whereas the non-coding 16S rRNA region was not partitioned. The model search for the ML analysis was performed with a greedy search algorithm (Schwarz 1978) and models were selected using the Akaike Information Criterion (AIC). ML analysis was performed using the web implementation of IQ-tree (Nguyen *et al*. 2015) under the following models of sequence evolution: GTR+F+I+G4 for partitions 1, 2, and TIM3+F+G4 for partition 3 of the ND2 gene and GTR+F+I+G4 for partition 4 of the 16S rRNA gene. The model of sequence evolution was determined using ModelFinder (Kalyaanamoorthy *et al*. 2017) on the IQ-tree web platform, and branch support was tested using 1000 non-parametric rapid ultrafast bootstrap pseudo-replicates (Minh *et al*. 2020). Mr Beast 2 (Bouckaert *et al*. 2019) was used to perform Bayesian inference (BI) for 16S rRNA. Bayesian posterior probabilities (BPP), the frequencies of nodal resolution, were estimated using a MCMC sampling approach after running one million atagenerations. The initial 20% of the samples were discarded as burnin. The tree containing all the species included in the analyses is given in Appendix 1.

Genetic divergence: The *p*-distances were calculated for the 16S rRNA gene in MEGA v.7. The substitution type was set as nucleotide, the model was kept as *p*-distance and the substitutions were included as d: Transitions + Transversions. Uniform rates were kept for analysis. Missing data were partially deleted and the site cutoff was set as 95%.

Results

***Phylogenetic relationship*.** The ML (16S + ND2) and the BI (16S) analysis shows the species to be a member of the *C. girii* clade (Fig. 1; Mirza *et al*. 2014; Sayyed *et al*. 2016, 2018, 2021; Khandekar *et al*. 2019, 2021a, b; Sayyed & Sulakhe 2020; Pal *et al*. 2021). The new species recovered is a sister to the *C. limayei*+*C. amba*+*C. girii*+*C. koynanensis*+*C. mahabali* clade with a high bootstrap (bp) support of 100 and a high posterior probability (pp) value of 1. Based on the uncorrected *p*-distance (Table 1), the new species was recovered nearest to *C. limayei* in the *C. girii* clade but can be separated with a genetic divergence of 3.8–8.4% on the 16S rRNA gene.

Table 1. Average pairwise uncorrected 16S sequence divergence% between new species, and other members of the *Cnemaspis girii* clade.

No	Species	1	2	3	4	5	6	7	8
1	*C. fortis* sp. nov.								
2	*C. mahabali*	3.8							
3	*C. limayei*	3.9	2.8						
4	*C. girii*	4.2	2.8	3.3					
5	*C. koynaensis*	5.1	3.4	3.1	2.5				
6	*C. rajgadensis*	6.2	5.1	6.3	6.5	6.7			
7	*C. ajijae*	6.8	5.9	7.1	6.5	7.6	1.9		
8	*C. flaviventralis*	8.4	8.9	8.5	8.4	9.0	6.1	7.8	

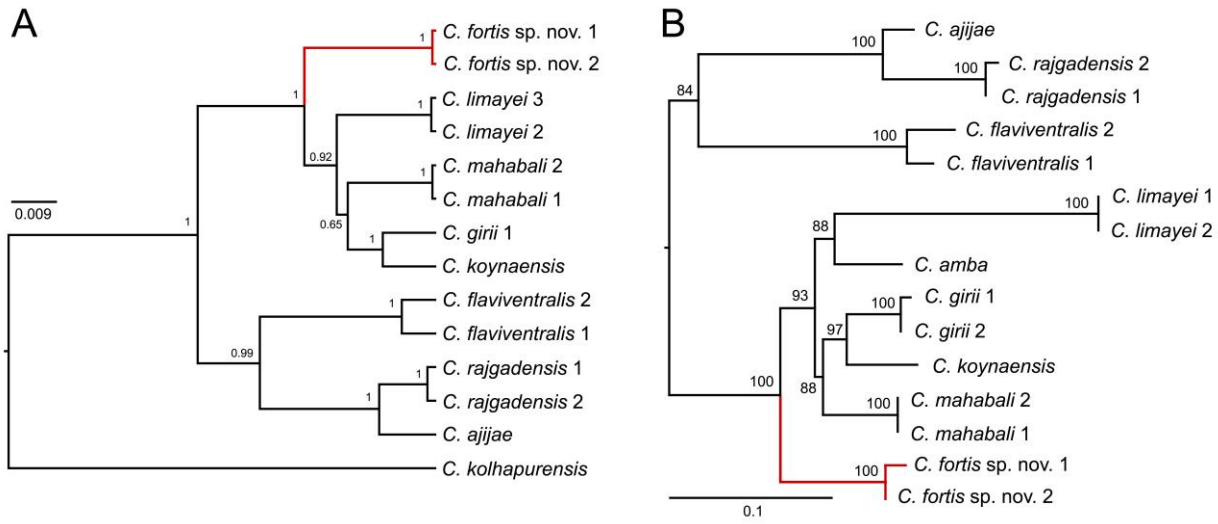

Figure 1. (A) BI phylogenetic tree based on 16S gene and **(B)** Maximum Likelihood phylogenetic tree based on 16S and ND2 concatenated dataset, showing the relationships among the species of the *Cnemaspis* from the *C. girii* clade. The values along the node represent the ultrafast bootstrap support for 1000 iterations.

Systematics

Cnemaspis fortis sp. nov.
[urn:lsid:zoobank.org:act: 805C1439-1ED3-4527-A934-FDA25E6DA2D5]
(Figs. 2–4, Tabel 2)

***Holotype*.** Adult male, BNHS 2925 (26.34 mm SVL), collected on the rock wall (18° 5' 12.2676" N 73° 24' 15.3072" E; ca. 45.3 m asl.) of Gandharpale Caves in Mahad, Maharashtra, India; collected by Amit Sayyed, Masum Sayyed and Ayaan Sayyed on 21 October 2021.

***Paratypes* (*n*=3).** Adult male BNHS 2926 (26.57 mm SVL), and BNHS 2927 (25.97 mm SVL), adult female BNHS 2928 (26.91 mm SVL), collection data same as holotype.

***Diagnosis*.** A small sized, *Cnemaspis* with adult SVL<27 mm (*n*=4); dorsal pholidosis heterogeneous; composed of circular, raised, granular scales intermixed with slightly enlarged, regularly arranged, weakly keeled, rounded tubercles, 11–12 longitudinal rows of enlarged tubercles; scales on snout and canthus rostralis large, round, juxtaposed, unkeeled, almost twice in size than those on forehead and interorbital region; scales on temporal region small, round, unkeeled, granular; scales on nape unkeeled, granular; scales on occiput unkeeled, granular, intermixed with slightly enlarged, randomly arranged, weakly keeled, rounded tubercles; scales on flanks small, granular, smooth, conical and spine-like tubercles absent on either side of the flanks; 7–8 supralabials; 7 infralabials; number of middorsal scales 63–65; rostral groove present, divided dorsally; mental enlarged, subtriangular, not pointed posteriorly; scales on ventral surface of neck, smooth, juxtaposed, weakly keeled; scales on chest, smooth, cycloid, feebly carinate; scales on ventral surface of abdomen between limb insertion smooth, cycloid; 136–150 longitudinal scales from mental to cloaca, midbody scales 33–35; subdigital lamellae under fourth digit of manus 12–13, under fourth digit of pes 12–14; males with 3–4 femoral pores on each thigh, separated medially by 19–24 poreless scales; dorsal scales of brachium keeled, imbricate, juxtaposed; dorsal scales of forearm keeled, imbricate, slightly smaller than those on brachials; dorsal scales of thigh and tibia imbricate, keeled; ventral scales of thigh flat, cycloid; ventral scales of tibia weekly keeled; dorsal scales at tail base granular, flatter, unkeeled intermixed with slightly enlarged keeled tubercles; dorsal scales on tail keeled, imbricate, intermixed with enlarged, slightly keeled, blunt, conical enlarged tubercles; enlarged tubercles on the tail forming whorls; median series slightly larger than rest; a single small, conical, postcloacal spur on each side.

Comparison. *Cnemaspis fortis* sp. nov. can be distinguished from all other Indian congeners on the basis of the following differing or non overlapping characters: small sized *Cnemaspis* range of SVL < 27 mm (vs. range of SVL > 30 mm in *C. aaronbaueri* Sayyed *et al*., 2019, *C. adii* Srinivasulu *et al*., 2015, *C. agarwali* Khandekar, 2019, *C. amboliensis* Sayyed *et al*., 2018, *C. fantastica* Agarwal *et al*., 2022, *C. flavigularis* Pal *et al*., 2021, *C. galaxia*

Pal *et al*., 2021, *C. goaensis* Sharma, 1976, *C. gracilis* (Beddome, 1870), *C. kalakadensis* Khandekar *et al*., 2022, *C. kolhapurensis* Giri *et al*., 2009, *C. mysoriensis* (Jerdon, 1853), *C. nigriventris* Pal *et al*., 2021, *C. pachaimalaiensis* Agarwal *et al*., 2022, *C. ranganaensis* Sayyed & Sulakhe, 2020, *C. reticulata* Sayyed *et al*., 2023, *C. uttaraghati* Khandekar *et al*., 2021, medium sized *Cnemaspis* SVL 40–50 mm in *C. anandani* Murthy *et al*., 2019, *C. balerion* Pal *et al*., 2021, *C. bangara* Agarwal *et al*., 2020, *C. boiei* (Gray, 1842), *C. chengodumalaensis* Cyriac *et al*., 2020, *C. graniticola* Agarwal *et al*., 2020, *C. heteropholis* Bauer, 2002, *C. jerdonii* (Theobald, 1868), *C. kolhapurensis*, *C. kottiyoorensis* Cyriac & Umesh, 2014, *C. lithophilis* Pal *et al*., 2021, *C. nairi* Inger *et al*., 1984, *C. nilagirica* Manamendra-Arachchi *et al*., 2007, *C. nimbus* Pal *et al*., 2021, *C. ornata* (Beddome, 1870), *C. thackerayi* Khandekar *et al*., 2019, *C. wallaceii* Pal *et al*., 2021, *C. wynadensis* (Beddome, 1870), *C. yelagiriensis* Agarwal *et al*., 2020, and large sized *Cnemaspis* SVL >50 mm in *C. anamudiensis* Cyriac *et al*., 2028, *C. beddomei* (Theobald, 1876), *C. maculicollis* Cyriac *et al*., 2018, *C. magnifica* Khandekar *et al*., 2020, *C. sisparensis* (Theobald, 1876), *C. smaug* Pal *et al*., 2021, *C. zacharyi* Cyriac *et al*., 2020); spine-like tubercles absent on flanks (vs. spine-like tubercles present on flanks in *C. agayagangai* Agarwal *et al*., 2022, *C. amboliensis*, *C. cavernicola* Khandekar *et al*., 2023, *C. fantastica*, *C. ganeshaiahi* Narayanan *et al*., 2023, *C. gracilis*, *C. goaensis*, *C. kalakadensis* Khandekar *et at*., 2022, *C. mundanthuraiensis* Khandekar *et al*., 2022, *C. monticola* Manamendra-Arachchi *et al*., 2007, *C. mundanthuraiensis*, *C. nicobaricus* Chandramouli, 2020, *C. pakkamalaiensis* Khandekar *et al*., 2023, *C. rudhira* Agarwal *et al*., 2022, *C. sakleshpurensis* Khandekar *et al*., 2022, *C. salimalii* Agarwal *et al*., 2022, *C. shevaroyensis* Khandekar *et al*., 2019, *C. stellapulvis* Khandekar *et al*., 2020, *C. tigris* Khandekar *et al*., 2022, *C. umashaankeri* Narayanan & Aravind, 2022, *C. vijayae* Khandekar *et al*., 2022); conical tubercles absent on flanks (vs. present in *C. anandani*, *C. andersonii* (Annandale, 1905), *C. assamensis* Das & Sengupta, 2000, *C. avasabinae* Agarwal *et al*., 2020, *C. azhagu* Khandekar *et al*., 2022, *C. jackieii* Pal *et al*., 2021, *C. jerdonii*, *C. krishnagiriensis* Agarwal *et al*., 2021, *C. magnifica*, *C. otai* Das & Bauer, 2000, *C. regalis* Pal *et al*., 2021, *C. schalleri* Khandekar *et al*., 2021, *C. shevaroyensis*, *C. thackerayi* Khandekar *et al*., 2019, and *C. yercaudensis* Das & Bauer, 2000); scales on ventral surface of neck and chest feebly carinate (vs. smooth in *C. aaronbaueri*, *C. adii*, *C. agarwali*, *C. ajijae*, *C. amba*, *C. amboliensis*, *C. australis* Manamendra-Arachchi *et al*., 2007, *C. avasabinae*, *C. azhagu*, *C. bangara*, *C. beddomei*, *C. boiei*, *C. chengodumalaensis*, *C. fantastica*, *C. flavigularis*, *C. galaxia*, *C. goaensis*, *C. gracilis*, *C. graniticola*, *C. heteropholis*, *C. indica* Gray, 1846, *C. kalakadensis*, *C. kolhapurensis*, *C. kottiyoorensis*, *C. maculicollis*, *C. magnifica*, *C. monticola*, *C. mysoriensis*, *C. nigriventris*, *C. pachaimalaiensis*, *C. palakkadensis* Sayyed *et al*., 2020, *C. ranganaensis*, *C. reticulata*, *C. uttaraghati*); scales on dorsal aspect of trunk heterogeneous (vs. scales on dorsal aspect of trunk homogeneous in *C. adii*, *C. assamensis*, *C. boiei*, *C. balerion*, *C. indica*, *C. jerdonii*, *C. kolhapurensis*, *C. littoralis* (Jerdon, 1853), *C. nilagirica, C. palakkadensis, C. palanica* Pal *et al*., 2021, *C. sisparensis*, *C. wynadensis*, and *C. zacharyi*); males with four femoral pores on each thigh, separated medially by 19–24 poreless scales (vs. femoral pores absent, only precloacal pores present in *C. aaronbaueri*, *C. anamudiensis*, *C. azhagu*, *C. beddomei*, *C. maculicollis*, *C. nairi*, *C. nimbus*, *C. ornata*, *C. regalis*, *C. rubraoculus* Pal *et al*., 2021, *C. smaug* and *C. wallaceii*; males with both femoral and precloacal pores present in *C. adii*, *C. agarwali*, *C. amboliensis*, *C. australis*, *C. avasabinae*, *C. cavernicola*, *C. bangara*, *C. goaensis*, *C. gracilis*, *C. graniticola*, *C. krishnagiriensis*, *C. mundanthuraiensis* Khandekar *et al*., 2022, *C. mysoriensis*, *C. otai*, *C. pakkamalaiensis*, *C. ranganaensis*, *C. rishivalleyensis*, *C. sakleshpurensis*, *C. schalleri*, *C. shevaroyensis*, *C. stellapulvis*, *C. thackerayi*, *C. yelagiriensis*, *C. yercaudensis* and *C. tigris*, *C. umashaankeri*, *C. vijayae*, *C. wicksi* (Stoliczka, 1873), and *C. yercaudensis*; 7–8 femoral pores in *C. sisparensis*, more than 12 femoral pores in males in *C. littoralis*, *C. palakkadensis*, *C. palanica*, both femoral and precloacal pores absent in *C. boiei*; a continuous series of 26–28 precloacal-femoral pores in *C. kolhapurensis*). Subcaudal scales smooth, median row slightly enlarged (vs. subcaudal scales smooth, median row distinctly enlarged in *C. aaronbaueri*, *C. agarwali*, *C. anandani*, *C. bangara*, *C. boiei*, *C. chengodumalaensis*, *C. gracilis*, *C. graniticola*, *C. heteropholis*, *C. indica*, *C. jerdonii*, *C. kolhapurensis*, *C. magnifica*, *C. nairi*, *C.*

nilagirica, *C. ornata*, *C. shevaroyensis*, *C. sisparensis*, *C. thackerayi*, *C. wynadensis*, *C. yelagiriensis*, *C. zacharyi*; median row of subcaudal scales slightly enlarged, without slightly larger scale alternating with a large divided scale in *C. amboliensis*, *C. avasabinae*, *C. goaensis*, *C. monticola*, *C. mysoriensis*, *C. otai*, *C. rishivalleyensis*, *C. stellapulvis* and *C. yercaudensis*).

Cnemaspis fortis sp. nov. closely resembles members of *girii* clade (*C. ajijae* Sayyed *et al*., 2018, *C. amba* Khandekar *et al*., 2019, *C. flaviventralis* Sayyed *et al*., 2016, *C. girii* Mirza *et al*., 2014, *C. koynaensis* Khandekar *et al*., 2019, *C. limayei* Sayyed *et al*., 2018, *C. mahabali* Sayyed *et al*., 2018, *C. rajgadensis* Sayyed *et al*., 2021 and *C. uttaraghati* Khandekar *et al*., 2021). However, it can be distinguished from all by having 33–35 midbody scales across the belly (vs. 29–30 midbody scales across the belly in *C. ajijae*, 22–24 in *C. amba*, 28–29 in *C. flaviventralis*, 26–28 in *C. girii*, 20–26 in *C. koynaensis*, 26–27 in *C. limayei*, 26 in *C. mahabali*, 28–29 in *C. rajgadensis* and 27–32 in *C. uttaraghati*); 11–12 paravertebral enlarged tubercles between forelimb and hindlimb insertions (vs. 17–22 paravertebral tubercles between forelimb and hindlimb insertions in *C. ajijae* and *C. amba*; 18 in *C. flaviventralis*, 20–22 in *C. girii*, 18–25 in *C. koynaensis* and 13–15 in C. *limayei* and 7–10 in *C. uttaraghati*); 136–150 longitudinal scales from mental to cloaca (vs. 141–149 longitudinal ventral scales from mental to cloaca in *C. amba*, 133–139 in *C. girii*, 123–141 in *C. rajgadensis*, 124–132 in *C. uttaraghati*); scales on ventral surface of neck and chest feebly carinate (vs. smooth in *C. amba*, *C. ajijae*, *C. flaviventralis*, *C. girii*, *C. koynaensis*, *C. limayei* and *C. uttaraghati*); subcaudal scales smooth, median row slightly enlarged, (vs. subcaudal scales smooth, median row not enlarged in, *C. amba*, *C. ajijae*, *C. flaviventralis*, *C. girii*, *C. limayei* and *C. koynaensis*); SVL up to 27 mm (vs. maximum SVL range in adults > 30 mm in *C. ajijae*, *C. amba*, *C. flaviventralis*, *C. girii*, *C. koynaensis*, *C. limayei* and *C. mahabali*); 16–17 lamellae under digit IV of manus (versus 15–16 lamellae under digit IV of manus in *C. ajijae*, *C. flaviventralis* and *C. mahabali*, 15 in *C. limayei* and 17–18 *C. uttaraghati*); dorsal scales on tail keeled, imbricate, intermixed with enlarged, slightly keeled, blunt, conical enlarged tubercles (vs. slightly enlarged, strongly keeled, conical enlarged tubercles *C. amba* and *C. koynaensis*, larger, posteriorly-pointed, subimbricate to imbricate, three sharply pointed, conical, keeled enlarged tubercles on dorsal tail present in *C. girii*, keeled, pointed enlarged tubercles in *C. mahabali* and enlarged, strongly keeled, distinctly pointed, conical tubercles in *C. uttaraghati*).

***Description of the holotype*.** An adult male generally in good state of preservation. 26.34 mm SVL, head short (HL/SVL 0.25), not depressed (HD/HL 0.45), slightly wide (HW/HL 0.69), distinctly larger from neck. Loreal region slightly inflated, canthus rostralis not prominent. Snout approximately half of head length (ES/HL 0.45); scales on snout and canthus rostralis large, round, juxtaposed, unkeeled, almost twice the size of those on forehead and interorbital region; scales on occipital and temporal region small, round, unkeeled, granular. Eye small (ED/HL 0.12), with round pupil; 14 supraciliaries, not elongate. Tympanum deep, ear opening rounded, smaller than head length (EOD/HL 0.07); eye to ear distance longer than diameter of eye (ET/EOD 4.38), ear opening approximately half of diameter of eye (EOD/ED 0.58). Rostral much wider (1.15 mm) than high (0.53 mm), divided dorsally, rostral groove present; enlarged supranasal on each side, twice the size of postnasals, divided in the middle by two small internasal scales; rostral in contact with supralabial I, nasal, internasal and supranasal; nostrils very small, oval, bordered by two postnasals, supranasal and rostral; three rows of small scales separate the orbit from the supralabials. Mental enlarged, subtriangular, not pointed posteriorly, longer (1.34 mm) than wide (1.10 mm); two pairs of postmentals, inner pair large, not connected with each other, separated by a large, hexagonal scale, posterior-postmentals small, postmentals bordered posteriorly by 10 smaller, rounded scales; gular scales small, granular, juxtaposed, smooth; scales on throat small, flat, juxtaposed, larger in size than those on gular. Supralabials up to angle of jaw seven on the right and eight on the left side; supralabial I slightly larger than II in size, not decreasing in size posteriorly; infralabials up to angle of jaw seven on the right and seven on the left side; infralabial I slightly larger than II in size. Canthal region with 13 scales on both sides; supraciliaries separated by 21 scales at midorbit.

Body relatively short, trunk less than half of SVL (AG/SVL 0.38) without ventrolateral folds. Dorsal pholidosis heterogeneous; composed of circular, raised, granular scales

intermixed with slightly enlarged, regularly arranged, weakly keeled, rounded tubercles, enlarged tubercles in 12 longitudinal rows, extending from limb insertion to tail; number of middorsal scales 63; scales on flanks small, granular, smooth, conical and spine-like tubercles absent on either side of the flanks. Granular scales on nape unkeeled, slightly smaller than those on paravertebral rows, scales on occiput unkeeled, similer in size to those on nape intermixed with slightly enlarged, randomly arranged, weakly keeled, rounded tubercles. Scales on ventral surface of neck, smooth, juxtaposed, feebly carinate; scales on chest, smooth, cycloid, feebly carinate; scales on ventral surface of abdomen between limb insertion smooth, cycloid; midventral scales 136, midbody scales 33 across the ventral between the lowest rows of dorsal scales; scales on femoral and precloacal region slightly larger than those on the abdomen; four femoral pores on either side of the thigh, separated medially by 22 poreless scales. Forelimbs moderately long, slender; dorsal scales of brachium keeled, imbricate, juxtaposed; dorsal scales of forearm keeled, imbricate, slightly smaller than those on brachials; ventral scales of brachium smooth, raised, granular smaller than those on forearm; scales beneath forearm, smooth, flat; palmar scales smooth, slightly raised; claws slightly recurved; dorsal scales of thigh and tibia imbricate, keeled; ventral scales of thigh flat, cycloid; ventral scales of tibia weekly keeled; plantar scales smooth, raised; lamellae beneath first phalanges slightly widened; subdigital lamellae on finger I: 9, finger II: 9, finger III: 12, finger IV: 12, finger V: 10; toe I: 9, toe II: 10, toe III: 13, toe IV: 13 and toe V: 13. Relative length of digits, fingers: IV (3.06 mm) >III (2.62 mm)>II (2.24 mm) >V (1.89 mm) >I (1.57 mm); toes: IV (3.39 mm) >III (2.95 mm) >V (2.47 mm) >II (2.27 mm) >I (1.46 mm).

Tail entire and original, cylindrical, moderately slender, flattened beneath, longer than snout–vent length (TL/SVL 1.25). Dorsal scales at tail base granular, similar in size and shape to those on midbody dorsum, gradually becoming larger, flatter, unkeeled intermixed with slightly enlarged, more larger than those on dorsal body, keeled tubercles; dorsal scales on tail keeled, imbricate, intermixed with enlarged, slightly keeled, blunt, conical enlarged tubercles; enlarged tubercles on the tail forming whorls, rest of the tail with decreased in size with paravertebral tubercles. Scales on ventral aspect of tail larger than those on dorsal aspect of tail, subimbricate, smooth; median series slightly larger than rest, regularly arranged; scales on tail base slightly smaller than those on midbody ventrals, smooth, imbricate; a single small, conical, postcloacal spur on each side.

Colouration of male in life (Fig. 4A)**.** The dorsal aspect of the head, lower body limbs and tail greyish brown intermixed with distinct small, yellow scattered, spots; occipital, neck and paravertebral region with white scattered, spots; yellow and black small markings on forehead and snout, supraciliaries brownish yellow; supralabial greyish brown with alternative brown and yellow spots; infralabials grey; a arrowhead marking dorsally between forelimb insertion; three black markings are present on the paravertebral region between limb insertions, with the third one having a half circular or horseshoe shape; the limbs are greyish brown above with irregular yellow and black markings; digits are grey with irregularly alternative yellow and black spots. Dorsal aspect of tail greyish brown with alternating white and black markings. The ventral side of the head, boday and tail white. Females have similar overall coloration.

Colouration of male in preservative (Figs 2, 3)**.** Dorsum of the head, body, limbs and tail with greyish brown which turns into dark brown, yellow and white markings and spots on dorsal head, body, limbs and tail which turns into grey, black markings remain black in preservation; ventral side of head, body, limbs and tail gray.

***Variation*.** Mensural and meristic data for the type series are given in Table 2. There are four specimens (three adult males and an adult gravid female) ranging in SVL from 25.97 mm to 26.91 mm. All paratypes resemble the holotype except as follows: the number of supralabials seven on the right side of the jaw in holotype, eight on each side in all paratypes; number of supraciliaries is 15 in holotype BNHS 2925, paratype BNHS 2927 male BNHS 2928 female, 14 in BNHS 2926; number of interorbital scales 27 in holotype BNHS 2925, 28 in paratype BNHS 2926 male and 29 in paratype BNHS 2927 male and BNHS 2928 female; the number of lamellae on digit I of the manus ranges from 8–9; the number of lamellae on digit IV of the manus from 12–13, lamellae on digit IV of the pes from 12–13; scales surrounded by the posterior-postmentals and between infralabials ranges from 9–11; number of midventral scales (MvS), from the first scale posterior to the

mental to last scale anterior to the vent; ventral scale counts in longitudinal series 136–150, and transverse series 33–35; number of middorsal scales ranges from 63–65; 4 femoral pores eachside present in holotype BNHS 2925 and paratype BNHS 2926, 3 in BNHS 2927. The three males and a female in our collection match in overall colouration with each other.

Table 2. Morphometric (in mm) and meristic data for the type series of *Cnemaspis fortis* sp. nov.; female paratype was gravid; + = broken tail.

Measurement	Male			Female
	Holotype BNHS 2925	Paratype BNHS 2926	Paratype BNHS 2927	Paratype BNHS 2928
snout–vent length (SVL)	26.34	26.57	25.97	26.91
axilla–groin length (AG)	10.10	10.28	10.03	10.95
trunk width (TW)	4.90	4.74	4.91	5.83
eye diameter (ED)	0.86	0.79	0.72	0.74
eye–nares distance (EN)	2.71	2.88	2.43	2.82
snout length (ES)	3.10	3.25	2.98	3.18
eye–ear distance (ET)	2.19	2.30	2.30	2.46
internarial distance (IN)	1.05	1.05	1.04	1.16
ear opening diameter (EOD)	0.50	0.50	0.48	0.51
head length (HL)	6.75	7.91	6.73	8.32
head width (HW)	4.68	4.73	4.60	4.57
head depth (HD)	3.10	3.29	2.99	2.67
interorbital distance (IO)	2.59	2.86	2.92	3.41
upper arm length (UAL)	2.50	2.50	2.47	2.72
lower arm length (LAL)	3.76	3.89	3.55	4.02
finger 1 length (FL 1)	1.57	1.47	1.52	1.72
finger 2 length (FL 2)	2.24	2.35	2.00	2.28
finger 3 length (FL 3)	2.62	2.71	2.48	2.59
finger 4 length (FL 4)	3.06	3.08	2.88	3.24
finger 5 length (FL 5)	1.89	2.01	2.02	2.40
femur length (FEL)	4.19	4.60	4.14	4.58
tibia length (TBL)	5.01	4.99	4.95	5.29
toe 1 length (TOL 1)	1.46	1.62	1.61	1.47
toe 2 length (TOL 2)	2.27	2.55	2.54	2.50
toe 3 length (TOL 3)	2.95	3.02	2.89	3.32
toe 4 length (TOL 4)	3.39	3.54	3.52	3.90
toe 5 length (TOL 5)	2.47	2.67	2.61	2.65
tail length (TL)	32.98	31.07	28.77	24.2+
supralabials (right/left)	7/8	8/8	8/8	8/8
infralabials (right/left)	7/7	7/7	7/7	7/7
supraciliaries	14	15	14	14
interorbital scales	27	28	29	29
scales between eye–tympanum	17	18	18	18
postnasals	2	2	2	2
postmentals	2	2	2	2
posterior postmentals	10	11	9	10
supranasals	2	2	2	2
canthal scales	13	13	14	14
midbody dorsal scale rows	63	64	65	64
dorsal tubercle rows	12	12	11	11
midventral scales	136	142	150	147
scale rows across the belly	33	35	34	33
femoral pores (right/left)	4/4	4/4	3/3	–
poreless scales	22	19	24	–
lamellae on distal digit (manus)	9/9/12/12/10	8/10/12/12/10	9/10/12/12/10	9/10/12/13/10
lamellae on distal digit (pes)	9/10/13/13/13	8/9/12/12/12	8/10/13/12/13	8/11/13/14/13
Subdigital lamellae finger IV	16	17	17	17

Plate 22

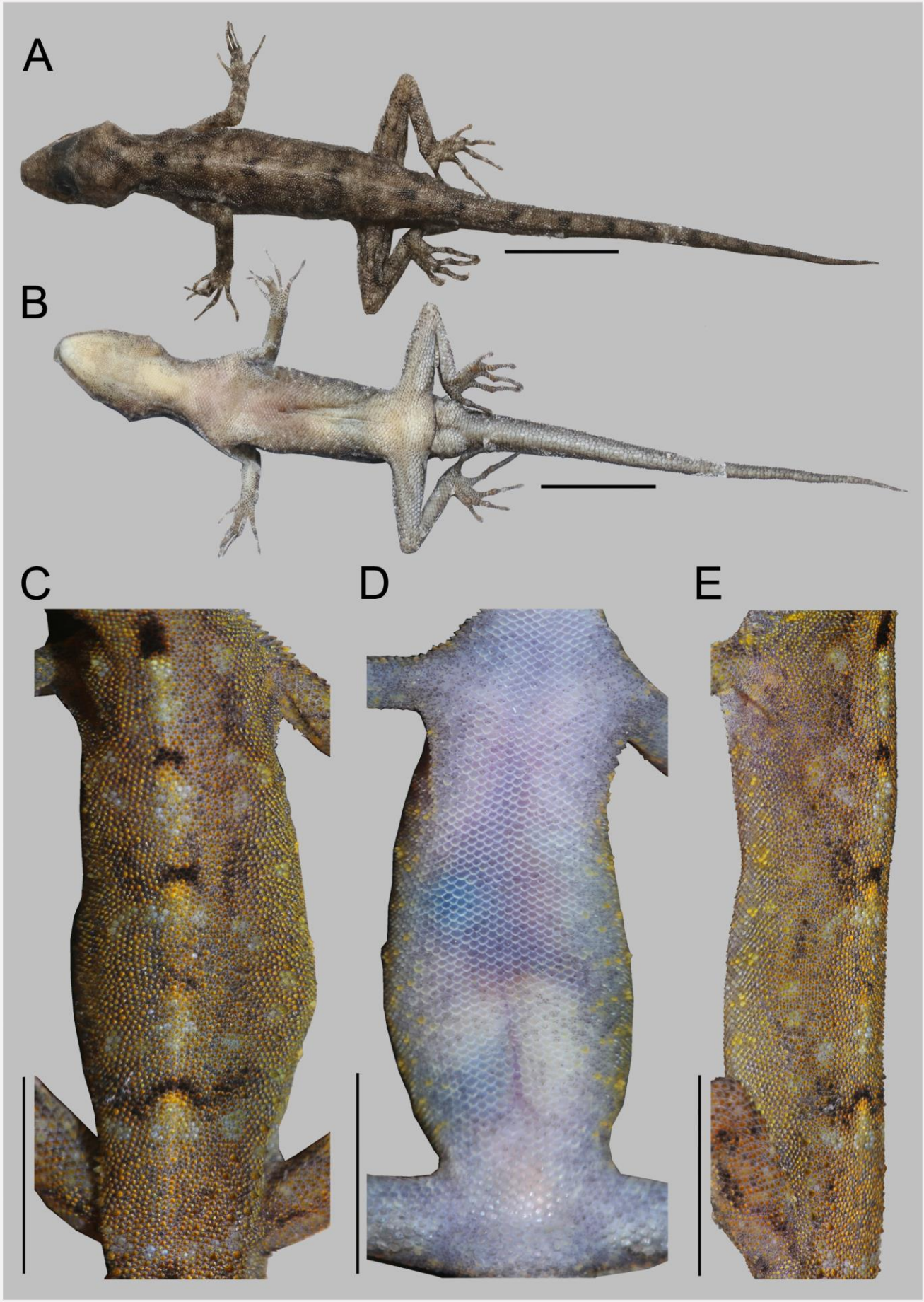

Figure 2. *Cnemaspis fortis* sp. nov. holotype (BNHS 2925): **(A)** dorsal and **(B)** ventral views of the body (scale: 10 mm); **(C)** dorsal, **(D)** ventral, and **(E)** lateral views of mid body (scale: 5 mm).

Plate 23

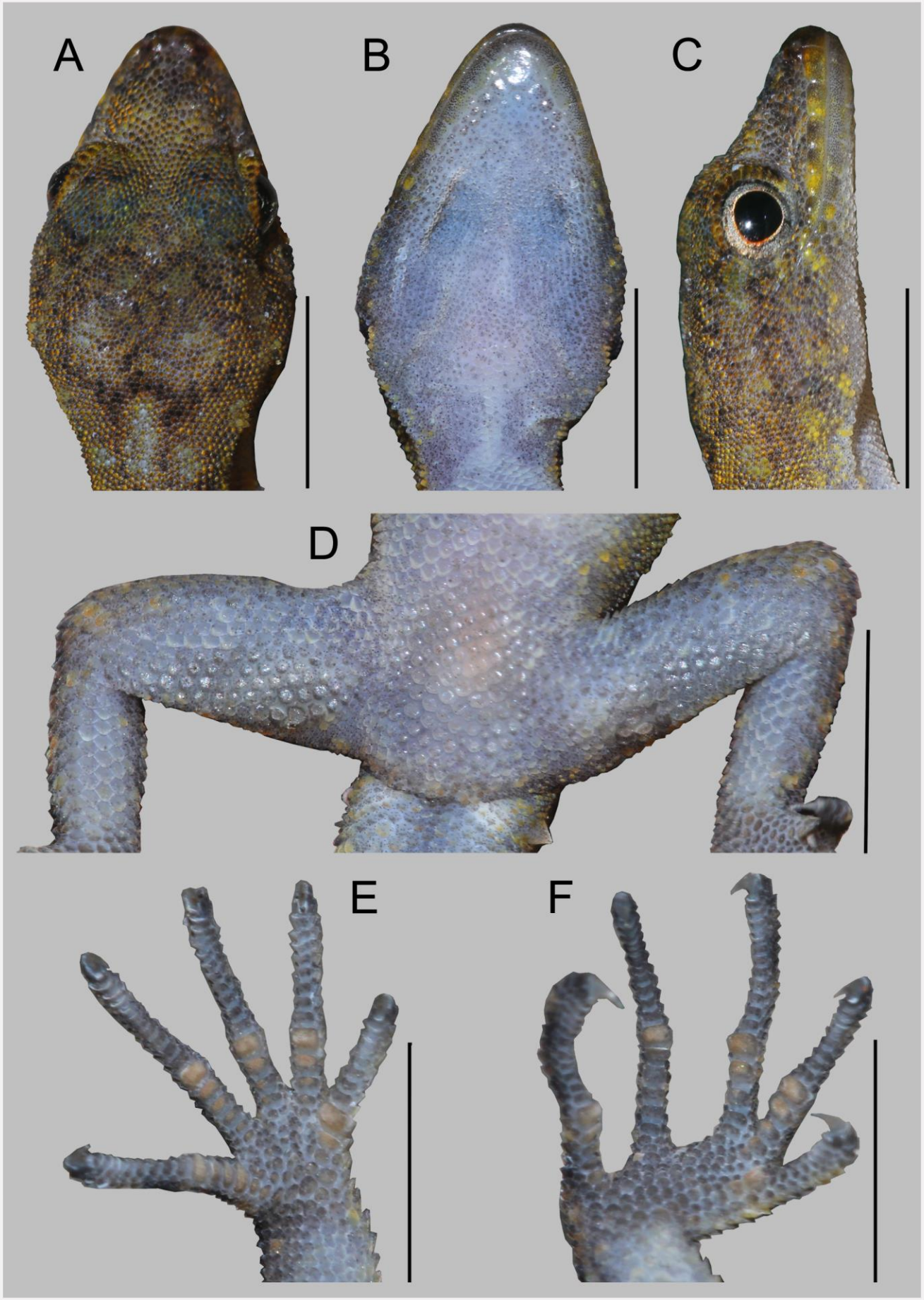

Figure 3. *Cnemaspis fortis* sp. nov. holotype (BNHS 2925): **(A)** dorsal, **(B)** ventral, and **(C)** lateral views of head; **(D)** femoral and precloacal region; and lamellae under **(E)** right menus and **(F)** right pes (scale 5 mm)

Plate 24

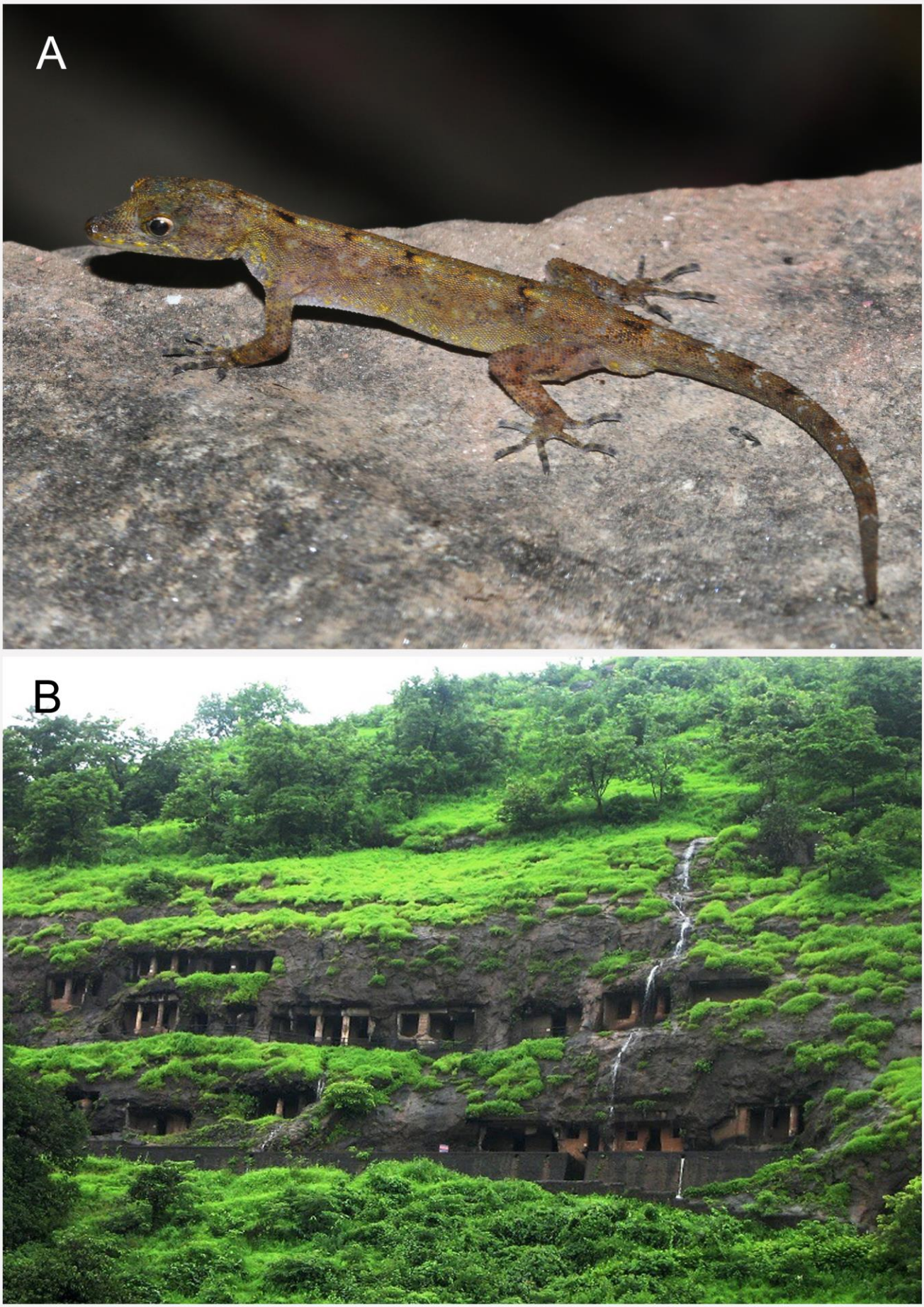

Figure 4. *Cnemaspis fortis* sp. nov. **(A)** holotype (male, BNHS 2925) in life; **(B)** habitat at the type locality (Gandharpale Caves in Mahad, Maharashtra, India).

***Etymology*.** The specific epithet "*fortis*" is a Latin third-declension adjective in the nominative singular given in feminine, refers to "strong" chosen to highlight the notable behaviour of bravery of the new species in its natural habitat. Suggested vernacular name is "brave dwarf gecko" in English.

***Natural History*.** During a visit to the Gandharpale Caves in Mahad (Fig. 4B), Maharashtra, India the individuals of the new species were encountered and collected. The new species was found on the basaltic wall of the cave. The caves are typically situated in a hilly and semi-evergreen forested area within the mountain range of the NWG of Maharashtra. The individuals were found dwelling on the rock walls both inside and outside of the caves. The behaviour of these geckos was found to be unexpected, as they displayed remarkable boldness and did not retreat far from humans at all. The new species was found to be sympatric with *Hemidactylus maculatus* Duméril & Bibron, 1836.

***Distribution*.** Currently, *Cnemaspis fortis* sp. nov., is known only from its type locality from Gandharpale Caves in Mahad, Maharashtra, India (Fig. 5).

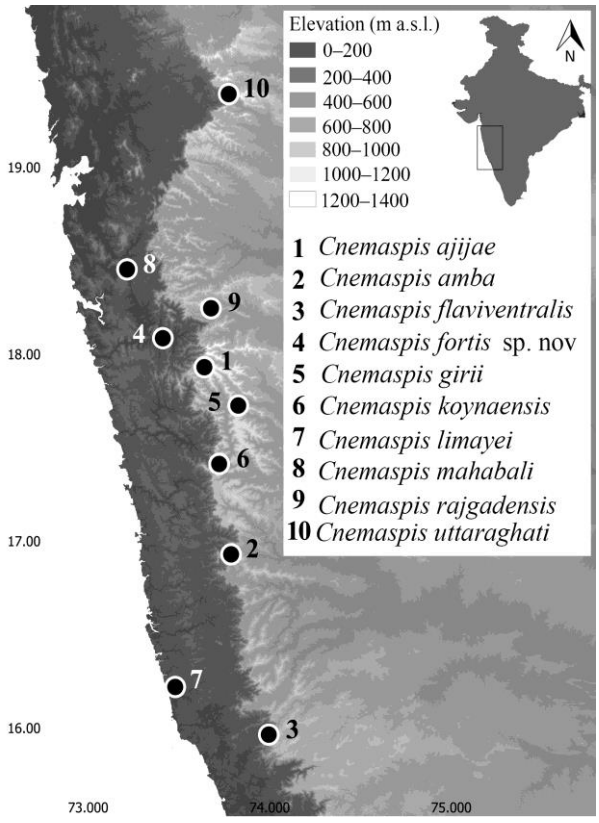

Figure 5. The map showing the distribution of the members of *C. girii* clade in the NWG of Maharashtra.

Discussion

This present study reports the discovery of one more new endemic species of *Cnemaspis* from the NWG of India, characterized by its diminutive size, with adult SVL measuring less than 27 mm. To date, this species represents the second smallest *Cnemaspis* found in India, the first being *C. rajgadensis*. The addition of *C. fortis* sp. nov. brings the total count of *Cnemaspis* in NWG to 14. *C. ajijae*, *C. amba*, *C. amboliensis*, *C. flaviventralis*, *C. girii*, *C. kolhapurensis*, *C. koynaensis*, *C. limayei*, *C. rajgadensis*, and *C. uttaraghati* are endemic to the NWG, whereas, *C. goaensis*, *C. mahabali*, and *C. ranganaensis* have a much wider distributional range within the region. Within the *Cnemaspis* genus, the "*girii*" clade, which includes *C. girii*, has garnered particular attention due to its unique evolutionary history and ecological adaptations. Potential barriers to gene flow, such as geographic features or ecological factors, have likely played a crucial role in shaping the diversity and distribution of the "*girii*" clade.

The NWG, recognized as a biodiversity hotspot, boasts a mosaic of diverse habitats, ranging from dense forests to open grasslands. This variety in habitat types, combined with the intricate topography of the region, has likely acted as a series of potential barriers for speciation within the "*girii*" clade. Mountains, rivers, and valleys can create isolation, limiting gene flow and facilitating the development of unique traits and adaptations. The varying ecological niches within this region, as well as the geographic isolation caused by the intricate terrain, have allowed for the evolution of numerous distinct species, each finely tuned to their particular habitat. The discovery of *C. fortis* sp. nov. underscores the ongoing need for research in this region, as it demonstrates that new species continue to be discovered, adding to the tapestry of biodiversity in the NWG.

As the study of *Cnemaspis* species, particularly within the "*girii*" clade, progresses, researchers will likely uncover more about the genetic relationships, ecological interactions, and the mechanisms that have driven the diversification within this fascinating group. This knowledge will enhance our understanding of the evolution of reptiles in the NWG and contribute to the broader field of herpetology. Conservation efforts must be prioritized to protect both the known and yet to be discovered species in this unique and fragile ecosystem.

Acknowledgements

I am grateful to S. Deshpande, S. Sulakhe and J. Purkayastha for their help in molecular work; A. Patki, D. Patki, M. Narwade, K. Salunkhe, S. Karjuljar, Y. Solankhe, D. Pawar, A. Varande and N. Guhagarkar (Wildlife Protection and Research Society, WLPRS) for their assistance during the fieldwork; Dr. Bhakre for his moral support; R. Khot (Deputy Director of BNHS, Mumbai) and O. Adhikari, for registration of the type specimens; Z.A. Mirza for valuable comments on the earlier draft; the WLPRS and Insearch Environmental Solutions (IES) for the laboratory facilities and institutional support;

Literature cited

Agarwal, I., A.M. Bauer, and T.R. Jackman (2016). A new species of *Cnemaspis* (Squamata: Gekkonidae) from the Western Ghats of Maharashtra, India. *Zootaxa*, 4170(2): 353–366.

Beddome, R.H. (1870). Descriptions of new reptiles from the Madras Presidency. *Madras Monthly Journal of Medical Science*, 2: 169–176.

Benson, D.A., M. Cavanaugh, K. Clark *et al*. (2017). GenBank. *Nucleic Acids Research*, 45(1): 37–42.

Bouckaert, R., T.G. Vaughan, J. Barido-Sottani *et al*. (2019). BEAST 2.5: An advanced software platform for Bayesian evolutionary analysis. *PLoS Computational Biology*, 15(4): e1006650.

Edgar, R.C. (2004). MUSCLE: Multiple sequence alignment with high accuracy and high throughput. *Nucleic Acids Research*, 32(5): 1792–1797.

Giri, V.B., A.M, Bauer, and K.S. Gaikwad (2009). A new ground-dwelling species of *Cnemaspis* Strauch (Squamata: Gekkonidae) from the northern Western Ghats, Maharashtra, India. *Zootaxa*, 2164 (1): 49–60.

Grismer, L.L., P.L. Wood, S. Anuar *et al*. (2014). Fossil herps and their terrestrial biodiversity from the Asian region. *Herpetological Conservation & Biology*, 9(1): 28–36.

Kalyaanamoorthy, S., B.Q. Minh, T.K.F. Wong *et al*. (2017). ModelFinder: Fast model selection for accurate phylogenetic estimates. *Nature Methods*, 14(6): 587–589.

Khandekar, A., T. Thackeray, and I. Agarwal (2019). Two more new species of *Cnemaspis* Strauch, 1887 (Squamata: Gekkonidae) from the northern Western Ghats, Maharashtra, India. *Zootaxa*, 4646(1): 236–250.

Khandekar, A., T. Thackeray, and I. Agarwal (2021a). A new species of day gecko (genus *Cnemaspis*) from the Western Ghats of Maharashtra, India. *Zootaxa*, 4968(3): 301–320.

Khandekar, A., T. Thackeray, and I. Agarwal (2021b). A novel small-bodied rupicolous *Cnemaspis* Strauch, 1887 (Squamata: Gekkonidae) from the northern Western Ghats, Maharashtra, India, with comments on the status of *C. indraneildasii*, Bauer 2000. *Zootaxa*, 4969(2): 331–350.

Kumar, S., G. Stecher, and K. Tamura (2016). MEGA7: Molecular evolutionary genetics analysis version 7.0 for bigger datasets. *Molecular biology & evolution*, 33(7): 1870–1874.

Leary, S., W. Underwood, R. Anthony, and S. Cartner (2013). *AVMA Guidelines for the Euthanasia of Animals*, 2013 edition. American Veterinary Medical Association, Illinois: 98pp.

Minh, B.Q., H.A. Schmidt, O. Chernomor *et al*. (2020). IQ-TREE 2: New models and efficient methods for phylogenetic inference in the genomic era. *Molecular Biology & Evolution*, 37(5): 1530–1534.

Mirza, Z.A., S. Pal, H.S. Bhosale, and R.V. Sanap (2014). A new species of gecko of the genus *Cnemaspis* Strauch, 1887 from the Western Ghats, India. *Zootaxa*, 3815(4): 494–506.

Myers, N., R.A. Mittermeier, C.G. Mittermeier *et al*. (2000). Biodiversity hotspots for conservation priorities. *Nature*, 403(6772): 853–858.

Narayanan, S. and N.A. Aravind (2022). A new species of rupicolous *Cnemaspis* Strauch, 1887 (Squamata: Gekkonidae) from the Biligirirangan Hills of Southern India. *Vertebrate Zoology*, 72: 823–837.

Narayanan, S., S. Pal, L.L. Grismer, and N.A. Aravind (2023). A new species of rupicolous *Cnemaspis* Strauch, 1887 (Squamata: Gekkonidae) from the Male Mahadeshwara Wildlife Sanctuary, southern Eastern Ghats, India. *Vertebrate Zoology*, 73: 189–203.

Nguyen, L.T., H.A. Schmidt, A. Von Haeseler, and B. Q. Minh (2015). IQ-TREE: A fast and effective stochastic algorithm for estimating maximum-likelihood phylogenies. *Molecular Biology & Evolution*, 32(1): 268–274.

Pal, S., Z.A. Mirza, P. Dsouza, and K. Shanker (2021). Diversifying on the ark: multiple new endemic lineages of dwarf geckos from the Western Ghats provide insights into the systematics and biogeography of South Asian

Cnemaspis (Reptilia: Squamata). *Zoological Research*, 42(6): 675–691.

Rodgers, W.A., H.S. Panwar, and V.B. Mathur (2000). *Wildlife Protected Area Network in India: A review, Executive summary*. Widlife Institute of India, Dehradun: 44pp.

Sayyed, A. and S. Sulakhe (2020). A new *Cnemaspis* Strauch, 1887 (Squamata: Gekkonidae) from the northern Western Ghats, Maharashtra, India. *Zootaxa*, 4885(1): 83–98.

Sayyed, A., R.A. Pyron, and N. Dahanukar (2016). *Cnemaspis flaviventralis*, a new species of gecko (Squamata: Gekkonidae) from the Western Ghats of Maharashtra, India. *Journal of Threatened Taxa*, 8(14): 9619–9629.

Sayyed, A., R.A. Pyron, and R. Dileepkumar (2018). Four new species of the genus *Cnemaspis* Strauch, (Sauria: Gekkonidae) from the northern Western Ghats, India. *Amphibian & Reptile Conservation*, 12(2): 1–29.

Sayyed, A., V.P. Cyriac, A. Pardeshi, and S. Sulakhe (2021). Dwarfs of the fortress: A new cryptic species of dwarf gecko of the genus *Cnemaspis* Strauch, 1887 (Squamata, Gekkonidae) from Rajgad fort in the northern Western Ghats of Maharashtra, India. *Evolutionary Systematics*, 5(1): 25–38.

Sayyed, A., S. Kirubakaran, R. Khot *et al*. (2023). A new rupicolous day gecko species (Squamata: Gekkonidae: *Cnemaspis*) from Tamil Nadu , south India. *Taprobanica*, 12(1): 5–13.

Schwarz, G. (1978). Estimating the dimension of a model. *The Annals of Statistics*, 6 (2): 461–464.

Sharma, R.C. (1976). Records of the reptiles of Goa. *Records of the Zoological Survey of India*, 71(1–4): 149–167.

Simon, C., A. Franke, and A. Martin (1991). The polymerase chain reaction: DNA extraction amplification. Pp. 329–355. *In:* Hewitt, G.M., A.W.B. Johnston, & J.P.W. Young. *Molecular Techniques in Taxonomy*. NATO ASI Series (Series H: Cell Biology), Volume 57. Springer, Berlin, Heidelberg.

Strauch, A.A. (1887). Bemerkungen über die Geckoniden-Sammlung im zoologischen Museum der kaiserlichen Akademie der Wissenschaften zu St. Petersburg. *Mémoires de l'Académie impériale des sciences de St. Pétersbourg*, ser. 7, 35(2): 1–72.

Tamura, K, and M. Nei (1993). Estimation of the number of nucleotide substitutions in the control region of mitochondrial DNA in humans and chimpanzees. *Molecular Biology & Evolution* 10(3): 512–526.

Appendix 1. List of GenBank accession numbers of ND2 and 16S sequences used in the analyses. Newly generated sequences in this study were deposited in the GenBank® nucleotide sequence database and are written in bold in the table.

No	Species	16S	ND2	Locality
1	*C. ajijae*	MZ291571	MZ701830	India, Maharashtra, Satara District, Mahabaleshwar
2	*C. amba*	–	MK792488	India, Maharashtra, Kolhapur District, Amba
3	*C. flaviventralis* 1	MZ291588	MZ701824	India, Goa
4	*C. flaviventralis* 2	KX269820	–	India, Maharashtra, Sindhudurg
5	*C. fortis* sp. nov. 1	**OR708519**	–	India, Maharashtra, Mahad, Gandharpale Caves
6	*C. fortis* sp. nov. 2	**OR708520**	–	India, Maharashtra, Mahad, Gandharpale Caves
7	*C. girii* 1	MZ291590	–	India, Maharashtra, Satara
8	*C. girii* 2	–	MK792491	India, Maharashtra, Satara
9	*C. kolhapurensis*	MZ291599	MZ701829	India, Maharashtra, Kolhapur District, Dajipur
10	*C. koynaensis*	–	MK792490	India, Maharashtra, Satara District, Humbarli
11	*C. limayei* 1	–	MK792482	India, Maharashtra, Kolhapur, Dajipur
12	*C. limayei* 2	MZ291601	–	India, Maharashtra, Kolhapur
13	*C. limayei* 3	KX753646	–	India, Maharashtra, Sindhudurg
14	*C. mahabali* 1	MZ291604	–	India, Maharashtra, Raigad
15	*C. mahabali* 2	MH174353	–	India, Maharashtra, Pune
16	*C. rajgadensis* 1	MW682866	–	India, Maharashtra, Pune, Rajgad
17	*C. rajgadensis* 2	MW682867	–	India, Maharashtra, Pune, Rajgad

Published date: 18 November 2023